Simulation of chaos-assisted tunneling in a semiclassical regime on existing quantum computers

A. D. Chepelianskii[1,2] and D. L. Shepelyansky[1]
[1]*Laboratoire de Physique Quantique, UMR 5626 du CNRS, Université Paul Sabatier, 31062 Toulouse Cedex 4, France*
[2]*Lycée Pierre de Fermat, Parvis des Jacobins, 31068 Toulouse Cedex 7, France*
(Received 20 February 2002; published 13 November 2002)

We present a quantum algorithm that allows one to simulate chaos-assisted tunneling in deep semiclassical regime on existing quantum computers. This opens additional possibilities for investigation of macroscopic quantum tunneling and realization of semiclassical Schrödinger cat oscillations [E. Schrödinger, Naturwissenschaften **32**, 807 (1935)]. Our numerical studies determine the decoherence rate induced by noisy gates for these oscillations and propose a suitable parameter regime for their experimental implementation.

DOI: 10.1103/PhysRevA.66.054301 PACS number(s): 03.67.Lx, 05.45.Mt, 75.45.+j

Since 1935 until recently, the metaphor of Schrödinger cat oscillations between life and death [1] was considered as a purely theoretical concept. However, during the last decade such oscillations in a quantum limit were observed for two states of a Rydberg atom in a quantum cavity [2] and an experimental evidence was presented for a quantum superposition of macroscopically distinct states in a superconducting quantum interference device (SQUID) [3]. Manifestations of macroscopic quantum tunneling (MQT) were also observed in magnetization experiments with spin-ten molecular magnets Fe_8 and Mn_{12} [4,5]. In addition to their fundamental interest, these experiments promise important applications, e.g., in solid-state qubit realization [6] and information storage [7] based on the Grover algorithm [8].

The regime discussed in Ref. [1] assumes that the quantum tunneling takes place for a semiclassical object with a regular dynamics in two symmetric regions of phase space. Recently, the investigations of quantum chaos led to an extension of this concept to the phenomenon of chaos-assisted tunneling between islands of regular integrable dynamics separated by a chaotic sea [9]. In this case, due to chaos the period T_u of tunneling oscillations becomes very sensitive to the variation of system parameters and statistical description should be used to describe the average distribution of T_u [9–11]. This unusual tunneling is strongly influenced by complex instanton orbits and scarring effects [10,11] and a chaos enhancement of tunneling rate by orders of magnitude may be reached by a small variation of parameters. The first direct experimental observations of the chaos-assisted tunneling have been realized recently with cold [12] and ultracold atoms from a Bose-Einstein condensate [13], thus opening more possibilities for the investigation of this interesting process. However, quantum tunneling is a very sensitive phenomenon, and experimental studies are complicated by the decoherence produced by the environment. Due to that, theoretical investigations of decoherence effects on MQT were initiated from the very beginning [14,15] and continue to date [16,17].

In this Brief Report, we show that quantum entanglement and quantum computer simulations [18] can be efficiently used to study quantum tunneling in deep semiclassical regime. We illustrate this on the example of a quantum symplectic map (double-well map) that has a rich phase-space structure with integrable islands surrounded by chaotic sea. Our algorithm has certain similarities with the algorithms for the kicked rotator [19] and for the sawtooth map [20]. It uses the quantum Fourier transform (QFT) [21] and simulates the dynamics of a quantum system with N levels in $O((\log_2 N)^4)$ operations per map iteration while any known classical algorithm requires at least $O(N\log_2 N)$ operations. Only one work space qubit is required for computations so that n_q qubits describe a physical system with $N=2^{n_q-1}$ levels. Contrary to Ref. [20], the present algorithm simulates the quantum dynamics with mixed (chaotic or integrable) classical phase space and is optimal for the investigation of chaos-assisted tunneling in semiclassical regime. Indeed, while for MQT in molecular magnets [4,5,22], the effective Planck constant $\hbar$ is inversely proportional to the number of spins ($\hbar \propto 1/n_q$) in our algorithm $\hbar \propto 2^{-n_q}$. Hence with only ten qubits, the algorithm allows one to study MQT with the semiclassical parameter being larger by almost two orders of magnitude. At present the nuclear-magnetic-resonance (NMR) quantum computer can perform QFT [23] and operate with up to seven qubits [24]. This allows one to study the chaos-assisted quantum tunneling on existing NMR based quantum computers and to obtain important information about decoherence effects in MQT regime.

In the classical limit, the dynamics of our model is described by the double-well map given by

$$\overline{p}=p-K\,dV(x)/dx,\quad \overline{x}=x+\overline{p}\pmod{2\pi}. \tag{1}$$

Here (p,x) are momentum and coordinate conjugated variables $(-\pi<x\leqslant\pi)$, the bars denote the variables after one map iteration, and $V(x)=(x^2-a^2)^2$. In the limit $K\to 0$, the map gives the one-dimensional integrable dynamics in the double-well potential $V(x)$ with the frequency of small oscillations $\omega_0=2\sqrt{2K}$. However, for $K>0$, the higher harmonics of finite step iterations lead to the appearance of chaotic component surrounding the stability islands located at $x=\pm a$. A typical example of the mixed phase space is shown in Fig. 1.

The quantum evolution on one map iteration is described by a unitary operator $\hat{U}$ acting on the wave function ψ:

$$\overline{\psi}=\hat{U}\psi=e^{-i\hat{p}^2/2\hbar}e^{-iKV(x)/\hbar}\psi, \tag{2}$$

where $\hat{p}=-i\hbar\,\partial/\partial x$ and $\psi(x+2\pi)=\psi(x)$. In the following we take the dimensionless $\hbar=4\pi/N$ that corresponds to the case of quantum resonance [25] with two classical cells (e.g.,

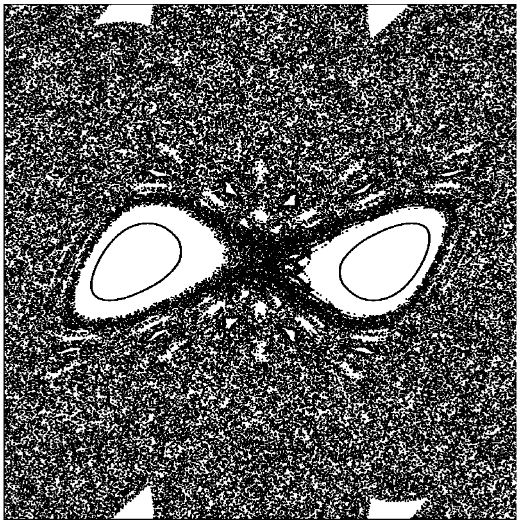

FIG. 1. Poincaré section for the double-well map (1) at $K=0.04$, $a=1.6$; one chaotic and two regular orbits are shown in the dimensionless cell $(-\pi\leqslant x,p\leqslant\pi)$.

as in Fig. 1) on a quantum torus containing N levels. The semiclassical regime corresponds to $\hbar \ll 1$ with discretized momentum $p=\hbar n$, where n is an integer. The most efficient known classical algorithm simulating the quantum dynamics (2) is based on forward/backward fast Fourier transform (FFT) between p and x representations. For a system with N levels it requires two FFT and two diagonal multiplications in p and x representations and can be performed in $O(N\log_2(N))$ operations.

The quantum algorithm simulates one map iteration (2) with $N=2^{(n_q-1)}$ levels in $O(n_q^4)$ quantum gates operating on n_q qubits with one qubit used as a work space. The initial wave function in the x representation is coded in the physical register with n_q-1 qubits in equidistant discrete points x_m $|\psi(x)\rangle=\sum_{m=0}^{N-1}a_m|m\rangle|0\rangle$ with an empty work n_q-th qubit. The action of kick $U_k=\exp[-iKV(x)/\hbar]$ is diagonal in this representation and the simultaneous multiplication of all N coefficients can be done in $3n_q^4$ gate operations. Indeed, if $x=\sum_{j=0}^{n_q-2}\alpha_j 2^j$, then $x^4=\sum_{j_1,j_2,j_3,j_4}\alpha_{j_1}\alpha_{j_2}\alpha_{j_3}\alpha_{j_4}2^{j_1+j_2+j_3+j_4}$ and $e^{-i\beta x^4}$

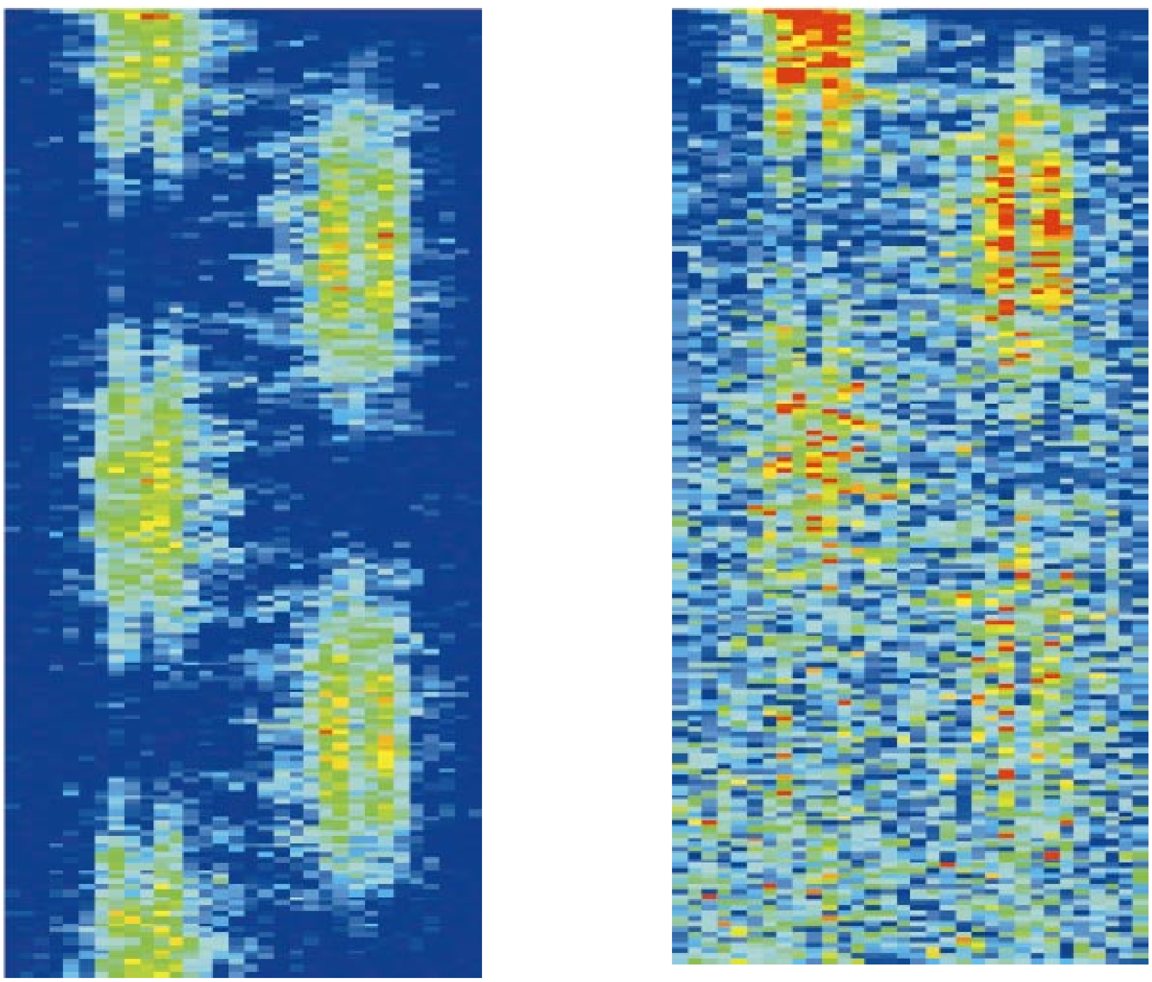

FIG. 2. (Color) Time evolution of the Schrödinger cat animated on a quantum computer: probability distribution $W(x)$ over the horizontal x axis for $-\pi\leqslant x\leqslant\pi$ is shown for different numbers of map iterations t, changing along vertical y axis from $t=0$ (top) to $t=180$ (bottom). Here as in Fig. 1, $K=0.04$, $a=1.6$, and $\hbar=4\pi/N$ with $N=2^{(n_q-1)}$. Quantum computation is done with $n_q=6$ qubits, ideal perfect gates (left) and noisy gates of strength $\epsilon=0.02$ (right), and $n_g=2090$ gates per one map iteration (2). At $t=0$, the initial coherent packet is located at $x=-a$. The color is proportional to the density: blue for zero and red for maximal density; axes are dimensionless.

$=\Pi_{j_1,j_2,j_3,j_4}\exp(-i\beta\alpha_{j_1}\alpha_{j_2}\alpha_{j_3}\alpha_{j_4}2^{j_1+j_2+j_3+j_4})$ with $\alpha_{j_{1,2,3,4}}=0$ or 1. This step can be performed with $\approx n_q^4$ four-qubit gates, namely, control-control-control–phase shift $[C^{(3)}(\beta)]$. The gate $C^{(3)}(\beta)$ is applied to each group of four qubits and transfers $|1111\rangle$ to $\exp(-i\beta 2^{j_1+j_2+j_3+j_4})|1111\rangle$ keeping other combinations unchanged. Using the work qubit, the gate $C^{(3)}(\beta)$ can be expressed via two Toffoli gates T and one control-control–phase shift $C^{(2)}(\beta)$ as $C^{(3)}_{j_1,j_2,j_3,j_4}(\beta)=T_{j_1,j_2,w}C^{(2)}_{w,j_3,j_4}(\beta)T_{j_1,j_2,w}$. Here the indices indicate the qubits on which the gates apply, β notes the rotation angle, and w is the work qubit, which is reset to zero after $C^{(2)}(\beta)$. Thus, the action of a kick is expressed via a sequence of standard gates used for quantum computations [21,26]. Indeed the Toffoli and $C^{(2)}(\beta)$ gates can be expressed via one- and two-qubit gates without addition of extra qubits [27]. The above computation is the most difficult step in the algorithm and takes $\approx 2n_q^4$ Toffoli gates and n_q^4 of $C(\beta)$ gates for large n_q. The multiplications by kick phases with lower powers of x are done in a similar way and require smaller number of gates. After multiplication by U_k, the algorithm is similar to the one used in Refs. [19,20]: the QFT changes the x representation to p representation in $O(n_q^2)$ operations, the rotation $U_\hbar=\exp(-i\hbar n^2/2)$ is realized in n_q^2 of control–phase-shift gates $C(\beta)$ and the backward QFT converts the wave function back to the initial x representation.

An example of the Schrödinger cat oscillations simulated by this quantum algorithm with ideal gates in the regime of chaos-assisted tunneling of Fig. 1 is shown in Fig. 2 (left). The time evolution of the probability distribution $W(x)$, integrated over the work qubit, shows clear tunneling transitions between the stability islands of Fig. 1. The same evolution simulated by noisy gates is illustrated in Fig. 2 (right). Noisy gates are modeled by unitary rotations by an angle randomly fluctuating in the interval $(-\epsilon/2,\epsilon/2)$ around ideal rotation angle. This noise introduces an effective decoherence rate Γ that destroys the tunneling oscillations after the time scale $1/\Gamma$.

To determine the period of tunneling oscillations T_u and their decay rate Γ, it is convenient to analyze the time dependence of total probability $W_a(t)$ at $x<0$ (see Fig. 3). The fit $W_a(t)-1/2\propto e^{-\Gamma t}\cos(2\pi t/T_u)$ allows one to obtain both T_u and Γ. We note that the value of W_a at given t can be obtained efficiently from few measurements, which enables one to determine T_u and Γ. Moreover, the values of T_u and Γ are not sensitive to the choice of the initial state at $t=0$. As it was discussed in Ref. [28] for a similar situation, this state should only have a sufficiently large overlap with the coherent state in the center of the stability island. For example, the step distribution, $W(x)=2/N$ for $x<0$ and $W(x)=0$ for $x>0$, which can be prepared efficiently, gives the same values of T_u and Γ as in the case of the coherent initial state.

The dependence of the decoherence rate on the parameters is shown in Fig. 4. The variation of Γ in a four-orders-of-magnitude range is well described by the relation

$$\Gamma=0.021\epsilon^2 n_q^4. \qquad (3)$$

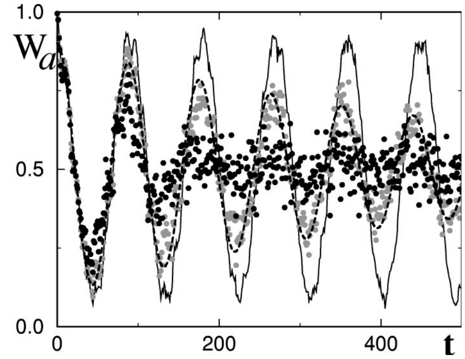

FIG. 3. Probability for the Schrödinger cat to be alive W_a (total probability for $x<0$) as a function of time t for parameters of Fig. 2. The time dependence allows one to determine the period of chaos-assisted tunneling oscillations $T_u=90$ and their decoherence decay rate Γ. The full curve shows the data without decoherence, points show the data for noisy gates with $\epsilon=0.01$ (gray) and $\epsilon=0.02$ (black). The fit of data (see text) gives $\Gamma=1.9\times10^{-3}$ (dashed curve for $\epsilon=0.01$). Time t is measured as the number of map iterations (dimesionless) and the probability is normalized to unity.

This relation can be understood using the following physical arguments. For a given qubit, noise in each unitary gate gives a drop of the probability to be directed along the ideal direction by an amount of ϵ^2. Since at each map iteration the number of gates is $n_g\sim n_q^4$, the total decay rate is proportional to $\epsilon^2 n_g$ in agreement with Eq. (3). We note that similar estimates for the decoherence rate induced by noisy gates were also obtained for the Shor algorithm [29]. At the same time the relation (3) is rather simple comparing to the decoherence rates discussed for MQT in SQUIDs [14–16] and molecular magnets [17]. One of the reasons for that is that the main step of the algorithm operates always with the same work qubit. If the unitary rotations of this qubit are noiseless, then the decay rate Γ is significantly reduced (see Fig. 4). Hence, the quantum error correcting codes [18] applied only

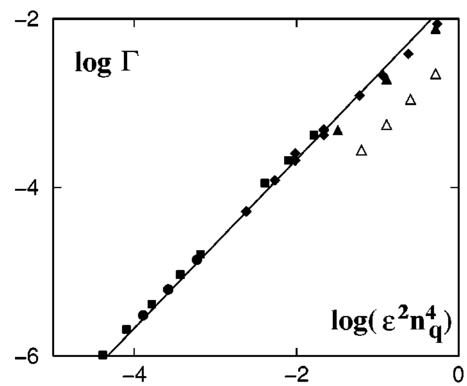

FIG. 4. Dependence of the decoherence rate of tunneling oscillations Γ on the strength of gate noise ϵ for different numbers of qubits $n_q=6$ (full triangles), 7 (diamonds), 8 (squares), and 9 (circles). The selected map parameters are varied in the range $1.4\leqslant a\leqslant1.7$, $0.04\leqslant K<0.06$ at $\hbar=\pi/2^{(n_q-3)}$ that gave the tunneling period variation in the range $90\leqslant T_u\leqslant1.8\times10^5$. The straight line shows the average dependence (3). The data with noiseless work qubit at $n_q=6$ ($K=0.04$, $a=1.6$) are shown by open triangles. Logarithms are decimal and all variables Γ,ϵ,n_q are dimensionless (Γ gives the decoherence rate per one map iteration).

to the work qubit can significantly reduce the decoherence rate, with a relatively small increase in the work space.

Our algorithm allows one to obtain interesting results about chaos-assisted tunneling even with a small number of qubits. For example, the data of Fig. 3 can be obtained experimentally on the basis of techniques applied in Refs. [23,24]. The main obstacle for experimental implementation of this algorithm is the decoherence. Indeed, to observe the Schrödinger cat oscillations, the decoherence time scale $1/\Gamma$ should be much larger than the oscillation period T_u. As it is usually the case for semiclassical tunneling, the later increases exponentially with the decrease of $\hbar$. This implies very rapid growth of T_u with n_q: $T_u \propto \exp(S/\hbar) \propto \exp(2^{n_q} S/8\pi)$, where $S \sim 1$ is a constant related to the classical action. For example, for $K=0.04$, $a=1.6$ the period changes from $T_u=90$ ($n_q=6$) to $T_u=1.68\times 10^6$ ($n_q=9$). Therefore even if the algorithm performs each map iteration (2) in polynomial number of gates, exponential number of map iterations should be done to observe tunneling oscillations in deep semiclassical regime. Nevertheless, in the regime of chaos-assisted tunneling, the value of S can be easily varied [9–11] by changing the parameters of the map (K and a) that allows one to obtain not-too-large T_u values for $n_q \leqslant 10$, e.g., $T_u=305$ for $K=0.3$, $a=0.5$, $n_q=10$. Indeed, the value of S can be changed significantly by reducing the size of the stability islands embedded in the chaotic sea. In spite of the rapid growth of T_u with the number of qubits n_q, the proposed algorithm uses them in an optimal way in order to reach the minimal effective Planck constant that scales as $\hbar \propto 2^{-n_q}$. This situation is qualitatively different comparing to SQUIDs [3] where even for a macroscopic number of particles (analogous to n_q) the evolution is described by a Hamiltonian with two levels and effective $\hbar \sim 1$ [16]. It also differs from the experiments [12,13] where effectively $\hbar \sim 1$ independently of the number of cold atoms.

In summary, our studies show that the Schrödinger cat can be animated in a deep semiclassical regime on existing quantum computers [23,24] with six or more qubits. Such experiments will give interesting information about the nontrivial regime of chaos-assisted tunneling in the presence of external decoherence. They will allow one to determine the effective accuracy of quantum computation, operability bounds, and decoherence rates for the first generation of quantum computers.

Note added: Recently the effects of decoherence in chaos-assisted tunneling were reported in experiments with cold cesium atoms [30].

This work was supported in part by the NSA and ARDA under ARO Contract No. DAAD19-01-1-0553, the NSF under Grant No. PHY99-07949, and the EC RTN Contract No. HPRN-CT-2000-0156.

[1] E. Schrödinger, Naturwissenschaften **32**, 807 (1935).
[2] J.M. Raimond, M. Brune, and S. Haroche, Rev. Mod. Phys. **73**, 565 (2001).
[3] J.R. Friedman, V. Patel, W. Chen, S.K. Tolpygo, and J.E. Lukens, Nature (London) **406**, 43 (2000).
[4] R. Sessoli, D. Gatteschi, A. Caneschi and A.M. Novak, Nature (London) **365**, 141 (1993).
[5] J.R. Friedman, M.P. Sarachik, J. Tejada, and R. Ziolo, Phys. Rev. Lett. **76**, 3830 (1996).
[6] Y. Nakamura, Y.A. Pashkin, and J.S. Tsai, Nature (London) **398**, 786 (1999).
[7] M.N. Leuenberger and D. Loss, Nature (London) **410**, 789 (2001).
[8] L.K. Grover, Phys. Rev. Lett. **79**, 325 (1997).
[9] O. Bohigas, S. Tomsovic, and D. Ullmo, Phys. Rep. **223**, 43 (1993).
[10] S.C. Creagh and N.D. Whelan, Phys. Rev. Lett. **84**, 4084 (2000).
[11] W.E. Bies, L. Kaplan, and E.J. Heller, Phys. Rev. E **64**, 016204 (2001).
[12] D.A. Steck, W.H. Oskay, and M.G. Raizen, Science **293**, 274 (2001).
[13] W.K. Hensinger, H. Häffner, A. Browaeys, N.R. Heckenberg, K. Helmerson, C. McKenzie, G.J. Milburn, W.D. Phillips, S.L. Rolston, H. Rubinsztein-Dunlop, and B. Upcroft, Nature (London) **412**, 52 (2001).
[14] A.O. Caldeira and A.J. Leggett, Phys. Rev. Lett. **46**, 211 (1981).
[15] A.J. Leggett, S. Chakravarty, A.T. Dorsey, M.P.A. Fisher, A. Garg, and W. Zwerger, Rev. Mod. Phys. **59**, 1 (1987).
[16] Y. Makhlin, G. Schön, and A. Shnirman, Rev. Mod. Phys. **73**, 357 (2001).
[17] E.M. Chudnovsky and X. Martines-Hidalgo, e-print cond-mat/0201184.
[18] For a review see, e.g., A. Steane, Rep. Prog. Phys. **61**, 117 (1998).
[19] B. Georgeot and D.L. Shepelyansky, Phys. Rev. Lett. **86**, 2890 (2001).
[20] G. Benenti, G. Casati, S. Montangero, and D.L. Shepelyansky, Phys. Rev. Lett. **87**, 227901 (2001)
[21] See, e.g., A. Ekert and R. Jozsa, Rev. Mod. Phys. **68**, 733 (1996).
[22] E.M. Chudnovsky and L. Gunther, Phys. Rev. Lett. **60**, 661 (1988).
[23] Y.S. Weinstein, M.A. Pravia, E.M. Fortunato, S. Lloyd, and D.G. Cory, Phys. Rev. Lett. **86**, 1889 (2001).
[24] L.M.K. Vandersypen, M. Steffen, G. Breyta, C.S. Yannoni, M.H. Sherwood, and I.L. Chuang, Nature (London) **414**, 883 (2001).
[25] F.M. Izrailev, Phys. Rep. **196**, 299 (1990).
[26] V. Vedral, A. Barenco, and A. Ekert, Phys. Rev. A **54**, 147 (1996).
[27] M. A. Nielsen and I. L. Chuang, *Quantum Computation and Quantum Information* (Cambridge University Press, Cambridge, 2000), p. 182.
[28] D.S. Abrams, and S. Lloyd, Phys. Rev. Lett. **83**, 5162 (1999).
[29] C. Miquel, J.P. Paz, and W.H. Zurek, Phys. Rev. Lett. **78**, 3971 (1997).
[30] D.A. Steck, W.H. Oskay, and M.G. Raizen, Phys. Rev. Lett. **88**, 120406 (2002).